

RU-96-12-B

A POSSIBLE MECHANISM FOR PSEUDO-GAP IN CUPRATES

Hai-cang Ren

Department of Physics, The Rockefeller University
New York, NY 10021-6399, U.S.A.

Abstract The electron spectrum in the normal phase of cuprates is analyzed in terms of the boson-fermion model. It is argued that the existence of the uncondensed pairs and the quasi-two-dimensional nature of the crystal structure are responsible for the pseudo-gap above T_C observed recently.

1. Introduction

Recently, ARPES experiments revealed a novel property of the underdoped cuprate superconductors in their normal phase. There is a pseudo-gap in the electron spectrum, i.e. a suppression of the spectral weight near the Fermi level above the transition temperature [1]. It is speculated by a number of authors that the phenomena may be attributed to the existence of the uncondensed pairs in the normal phase. The present article is an attempt in this direction.

A common feature of the cuprate superconductors is that the coherence length is comparable with the lattice spacing on the CuO_2 plane. Therefore the Cooper pairs, if they exist, are highly localized in the coordinate space and consequently can be regarded as boson degrees of freedom. The superconductivity is thereby associated with the kinematical Bose-Einstein condensation of these pairing states and there must be uncondensed pairs in the normal phase.

The crystal structure of all cuprate materials is highly anisotropic. It consists of parallel layers of CuO_2 , the minimum distance between oxygens (where the doped charge carriers may reside) on the same layer is less than 3\AA . The separations between neighboring CuO_2 layers are not even but periodic with an average spacing around 6\AA . The

number of layers in each period varies from one for $La_{2-x}Sr_xCuO_4$ ($T_C \leq 40K$) to three for $Tl_2Ca_2Ba_2Cu_3O_x$ ($T_C \leq 120K$). Although the coherence perpendicular to the CuO_2 layer is required for the condensate to form below T_C , the normal phase properties of the under-doped materials are largely two dimensional in nature. This has been confirmed by a number of experiments on the transport coefficients of cuprates [2].

The Bose-Einstein condensation is characterized by the relation that the thermal wavelength of the bosons,

$$\lambda_T = \sqrt{\frac{2\pi}{m_b \kappa T}} \quad (1.1)$$

with m_b the effective mass of bosons, at the transition temperature $T = T_C$ should be comparable with the inter-boson distance, l , so that quantum mechanical coherence takes place. The ratio $\frac{\lambda_T}{l}$ is 1.38 for an ideal Bose gas and 1.65 for $HeII$ at the λ -transition. For high T_C materials, the ratio

$$\frac{\lambda_{T_C}}{l} \sim 2.8 \quad (1.2)$$

was estimated in [3] based on the results of the μSR experiment [4]. The reasoning went as follows: According to the experimental results, the transition temperature T_C of the under-doped material is inversely proportional to the square of the magnetic penetration depth with a constant of proportionality universal for all cuprates. If the supercurrent is identified with the superfluid of bosons. A relation

$$T_C(K) = 10^5 \frac{m_e}{m_b} \frac{n_b}{d} \quad (1.3)$$

was obtained, where m_e is the electron mass in vacuum, m_b is the in-plane effective mass of the bosons, n_b is the density of the bosons (counted as number of bosons per \AA^2 and per layer) and d the average separation between CuO_2 layers (in the unit of \AA). Combining the relation (1.3) with $d = 6\text{\AA}$, $n_b = l^{-2}$ and the definition of the thermal wavelength (1.1), the ratio (1.2) follows independent of m_b . This ratio is certainly consistent with the picture of Bose-Einstein condensation.

In an isotropic situation, a relation $\lambda_{T_C} \sim l$ implies $T_C \propto n_b^{\frac{2}{3}}$ in accordance with (1.1) and $n_b = l^{-3}$. This is not the case of (1.3). Therefore we have to resort to the quasi-two dimensional layer structure of the system. Consider an ideal Bose gas in quasi-two dimensions

whose kinetic energy consists a free motion term in $x - y$ plane and a hopping(tunneling) term in z -direction, i.e.

$$\omega_{\vec{p},K} = \frac{p^2}{2m_b} + 2t_b(1 - \cos Kd), \quad (1.4)$$

where \vec{p} is the momentum in $x - y$ plane, K is the Bloch momentum in z -direction and t_b is the out-of-plane hopping amplitude. Expanding the cosine of (1.4) to K^2 term, we obtain the out-of-plane effective mass

$$M_b = (2t_b d^2)^{-1} \quad (1.5)$$

The density of states of the spectrum (1.4) is

$$\rho(\omega) = \frac{m_b}{2\pi} \begin{cases} \frac{1}{\frac{2}{\pi} \sin^{-1} \sqrt{\frac{\omega}{4t_b}}} & \text{for } \omega > 4t_b; \\ \frac{2}{\pi} \sin^{-1} \sqrt{\frac{\omega}{4t_b}} & \text{for } \omega < 4t_b. \end{cases} \quad (1.6)$$

The boson density (counted as number of bosons per unit area and per layer) at a temperature T and a chemical potential $\mu < 0$ is

$$n_b = \int_{-\pi}^{\pi} \frac{d\theta}{2\pi} \int \frac{d^2p}{(2\pi)^2} \frac{1}{e^{\beta(\omega-\mu)} - 1} = \frac{1}{\lambda_T^2} \int_{-\pi}^{\pi} \frac{d\theta}{2\pi} \ln \frac{1}{1 - e^{-\beta[2t_b(1-\cos\theta)-\mu]}}, \quad (1.7)$$

where $\beta = \frac{1}{\kappa T}$, and $\lambda_T = \sqrt{\frac{2\pi}{m_b \kappa T}}$ is the thermal wavelength of the bosons in the $x - y$ plane. For $\beta t_b \ll 1$ and $-\beta\mu \ll 1$, the integral (1.7) may be expressed in terms of elementary functions. We find that

$$n_b = \frac{1}{\lambda_T^2} \ln \frac{2\kappa T}{(2t_b - \mu) + \sqrt{(2t_b - \mu)^2 - 4t_b^2}}. \quad (1.8)$$

At the transition $\mu = 0$ and we have

$$n_b = \frac{1}{\lambda_{T_C}^2} \ln \frac{\kappa T_C}{t_b} = \frac{m_b \kappa T_C}{2\pi} \ln \frac{\kappa T_C}{t_b}. \quad (1.9)$$

Regarding $x - y$ plane as a CuO_2 layer, it was found in [5] that this quasi-linear relation between n_b and T_C fits the μSR result (1.3) remarkably well with

$$\ln \frac{\kappa T_C}{t_b} \sim 8 \text{ at } T_C = 100K, \quad (1.10)$$

which implies that

$$t_b/\kappa T_C = 3.6 \times 10^{-4}. \quad (1.11)$$

Furthermore, the formula (1.10) can be generalized to the material with multi-layers in a period in z direction provide we replace the hopping amplitude t_b in (1.10) by the geometrical mean of the hopping amplitudes between each pair of neighboring layers within one period. This also explains the universality of the $n_b - T_C$ profile (1.3), since the tunneling nature of boson motion in z -direction makes the geometrical mean of the hopping amplitudes sensitive only to the average separation between the CuO_2 layers and this average is approximately the same for different cuprates.

The large logarithmic factor is obviously caused by the large fluctuations of low-lying bosons, i.e. the $2D$ nature of the density of state (1.6) down to the tiny energy scale t_b . Since the square root of the logarithm of (1.10) gives the quoted ratio (1.2), the quasi-two-dimensional character also responsible for the factor two enlargement of this ratio compared with that of an ideal Bose gas in three dimensions, bearing in mind that within $3D$, the change of this ratio from an ideal Bose gas to the highly interaction $HeII$ is merely 20%.

A simple phenomenological model dealing with system with localized Cooper pairs was proposed in [3] and [6], which will be referred to as the boson-fermion model. In the rest of the paper, we shall first review this model and then apply it to explore the consequences of the presence of uncondensed bosons within a quasi-two-dimensional crystal in the normal phase.

2. The Boson-Fermion Model in Quasi-Two Dimensions

The boson-fermion model appropriate to the quasi-two dimensional crystal structure is formulated in ref.[7]. The grand Hamiltonian of the system reads

$$H = \sum_{\vec{P},s} \epsilon_{\vec{P}} a_{\vec{P}s}^\dagger a_{\vec{P}s} + \sum_{\vec{P}} \omega_{\vec{P}} b_{\vec{P}}^\dagger b_{\vec{P}} + \frac{g}{\sqrt{N\Omega}} \sum_{\vec{P},\vec{Q}} (b_{\vec{P}} a_{\frac{\vec{P}}{2} + \vec{Q}\uparrow}^\dagger a_{\frac{\vec{P}}{2} - \vec{Q}\downarrow}^\dagger + b_{\vec{P}}^\dagger a_{\frac{\vec{P}}{2} - \vec{Q}\downarrow} a_{\frac{\vec{P}}{2} - \vec{Q}\uparrow}), \quad (2.1)$$

where $a_{\vec{P}s}$ and $a_{\vec{P}s}^\dagger$ ($b_{\vec{P}}$ and $b_{\vec{P}}^\dagger$) are annihilation and creation operators of electrons (bosons), the subscript s denotes the spin orientation

($s = \uparrow$ or \downarrow),

$$\epsilon_{\vec{P}} = \frac{p^2}{2m_f} + 2t_f(1 - \cos Kd) - \mu, \quad (2.2)$$

$$\omega_{\vec{P}} = \frac{p^2}{2m_b} + 2t_b(1 - \cos Kd) + 2(\nu - \mu), \quad (2.3)$$

$m_f(m_b)$ is the in-plane effective mass of electrons(bosons), $t_f(t_b)$ is the out-of-plane hopping amplitude of fermions(bosons), μ is the chemical potential of the system, 2ν is the energy of a static boson relative to two static electrons ($2\nu = \omega_{\vec{P}}|_{\vec{P}=0} - 2\epsilon_{\vec{P}}|_{\vec{P}=0}$), Ω is the total area of a CuO_2 layer and \mathcal{N} is the total number of layers of the whole system. The vectors with capital symbols, \vec{P} and \vec{Q} are all three dimensional, i.e.

$$\vec{P} = \vec{p} + K\hat{z}$$

and

$$\vec{Q} = \vec{q} + K'\hat{z}$$

with \vec{p} , \vec{q} parallel to the $x - y$ plane, K , K' Bloch momenta in z direction whose value varies between $-\pi/d$ and π/d . The conserved electric charge is given by

$$N = \sum_{\vec{P},s} a_{\vec{P}s}^\dagger a_{\vec{P}s} + 2 \sum_{\vec{P}} b_{\vec{P}}^\dagger b_{\vec{P}}. \quad (2.4)$$

For resonant bosons, $\nu > 0$ and the dimensionless coupling constant g is related to the boson width in vacuum through

$$\Gamma = \frac{g^2}{4} m_f \begin{cases} 1 & \text{for } \nu > 4t_f; \\ \frac{2}{\pi} \sin^{-1} \sqrt{\frac{\nu}{4t_f}} & \text{otherwise.} \end{cases}$$

For $g = 0$, the model implies an ideal Bose gas and an ideal fermion gas in chemical equilibrium. In what follows we shall assume that $\nu > 4t_f$. The effective expansion parameter of the perturbation series is \hat{g} defined by

$$\hat{g}^2 = \frac{\Gamma}{\nu} = g^2 \frac{m_f}{4\nu}. \quad (2.5)$$

The condensation mechanism with resonance bosons can be understood easily in the weak coupling limit, $\hat{g} \ll 1$ and at $T = 0$. Starting with low charge density, the fermionic levels $\epsilon_{\vec{P}}$ are filled first. The bosons are unstable, existing in virtual state through the interaction and the condensate is of BCS type. With the increasing

charge density, the fermion levels are filled up to ν . Additional charges will be stabilized at the zero momentum boson level to minimize the energy since the decay channels of a static bosons are all locked by the Fermi sea and the condensate is of Bose-Einstein type.

In the super-phase, we introduce a long range order B representing the Bose condensate at the $\vec{P} = 0$, i.e.

$$b_{\vec{P}}|_{\vec{P}=0} = \sqrt{\Omega}Be^{i\alpha} + b', \quad (2.6)$$

where $B > 0$, α is a constant phase, and then

$$H = H_0 + H_1, \quad (2.7)$$

$$\begin{aligned} H_0 &= 2\Omega(\nu - \mu) + \sum_{\vec{P}} \omega_{\vec{P}} b_{\vec{P}}^\dagger b_{\vec{P}} \\ &+ \sum_{\vec{P}} [\epsilon_{\vec{P}} (a_{\vec{P}\uparrow}^\dagger a_{\vec{P}\uparrow} + a_{\vec{P}\downarrow}^\dagger a_{\vec{P}\downarrow}) + \Delta (e^{i\alpha} a_{\vec{P}\uparrow}^\dagger a_{-\vec{P}\downarrow}^\dagger + e^{-i\alpha} a_{-\vec{P}\downarrow} a_{\vec{P}\uparrow})] \end{aligned} \quad (2.8)$$

with $\Delta = gB$, and H_1 includes the cubic terms in a 's and b 's. The electron spectrum to the zeroth order in H_1 but to all orders in Δ can be obtained via a Bogoliubov transformation of H_0 . In order to compare notes with the normal phase results later on, we adapt diagrammatic technique to derive the electron spectrum. All the diagrams throughout this paper are thermal with discrete imaginary energies (Matsubara variables) and continuous spatial momenta. The real-time (real energy) Green's functions can be obtained by replacing all external Matsubara energies by real and continuous energies. The uniqueness of such a replacement was established in [8].

Returning to H_0 , we associate a solid line with the bare electron propagator

$$\frac{i}{i\nu_n - \epsilon_{\vec{P}}} \quad (2.9)$$

with $\nu_n = \frac{2\pi}{\beta}(n + \frac{1}{2})$ and $\epsilon_{\vec{P}}$ given by (2.2), a cross with two incoming fermion lines is associated with a factor $-i\Delta$ and that with two outgoing lines with a factor $i\Delta$. The electron propagator to all orders in Δ but to zeroth order in H_1 (represented by a solid line with two arrows), with a momentum \vec{P} and a discrete energy $i\nu_n$, $S_n(\vec{P})$, corresponds to the sum of the diagrams in Fig.1.

We have

$$S_n(\vec{P}) = \frac{i}{i\nu_n - \epsilon_{\vec{P}}} \sum_{N=0}^{\infty} (-i\Delta)^N (i\Delta)^N \left(\frac{i}{-i\nu_n - \epsilon_{\vec{P}}} \right)^N \left(\frac{i}{i\nu_n - \epsilon_{\vec{P}}} \right)^N$$

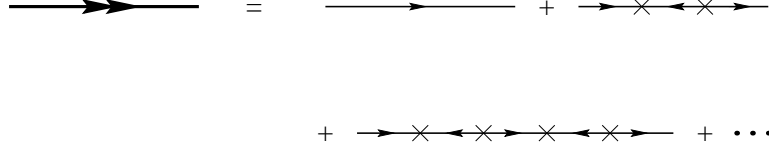


Figure 1. The diagrammatic expansion of the electron propagator in the super phase

$$= \frac{\nu_n - i\epsilon_{\vec{P}}}{\nu_n^2 + E_{\vec{P}}^2} \quad (2.10)$$

where $E_{\vec{P}} = \sqrt{\epsilon_{\vec{P}}^2 + \Delta^2}$. Replacing the Matsubara energy $i\nu_n$ by $p_0 + i0^+$ with p_0 real, we obtain the retarded electron propagator

$$S_R(p_0, \vec{P}) = \frac{i(p_0 + \epsilon_{\vec{P}})}{(p_0 + i0^+)^2 - E_{\vec{P}}^2}. \quad (2.11)$$

The corresponding spectral density is

$$A(p_0, \vec{P}) \equiv \frac{1}{\pi} \text{Re} S_R(p_0, \vec{P}) = \frac{|p_0 + \epsilon_{\vec{P}}|}{2E_{\vec{P}}} [\delta(p_0 - E_{\vec{P}}) + \delta(p_0 + E_{\vec{P}})] \quad (2.12)$$

with two infinitely sharp quasi-particle peaks. On writing

$$S(p_0, \vec{P}) = \frac{i}{p_0 + i0^+ - \epsilon_{\vec{P}} - \Sigma(p_0 + i0^+, \vec{P})} \quad (2.13)$$

we extract the self-energy function

$$\Sigma(p_0, \vec{P}) = \frac{\Delta^2}{p_0 + \epsilon_{\vec{P}}} \quad (2.14)$$

3. The Electron Self-Energy in the Normal Phase

Above the transition temperature, $T > T_C$, the coherence between different layers is no longer crucial and we shall approximate the model Hamiltonian (2.1) by a purely two-dimensional one, i.e.

$$H = \sum_{\vec{p}, s} \epsilon_{\vec{p}} a_{\vec{p}s}^\dagger a_{\vec{p}s} + \sum_{\vec{p}} \omega_{\vec{p}} b_{\vec{p}}^\dagger b_{\vec{p}}$$

$$+\frac{g}{\sqrt{\Omega}} \sum_{\vec{p},\vec{q}} (b_{\vec{p}} a_{\frac{\vec{p}}{2}+\vec{q}\uparrow}^\dagger a_{\frac{\vec{p}}{2}-\vec{q}\downarrow}^\dagger + b_{\vec{p}}^\dagger a_{\frac{\vec{p}}{2}-\vec{q}\downarrow} a_{\frac{\vec{p}}{2}+\vec{q}\uparrow}), \quad (3.1)$$

where

$$\epsilon_{\vec{p}} = \frac{p^2}{2m_f} - \mu, \quad (3.2)$$

$$\omega_{\vec{p}} = \frac{p^2}{2m_b} + \delta \quad (3.3)$$

with $\delta = 2(\nu - \mu)$ whose value in the vicinity above T_C is regarded of the same order of t_b in (1.11). All momenta are two-dimensional from now on.

3.1 The self-energy to one-loop order

In terms of the thermal diagrams, a free electron propagator, represented by a solid line, with a momentum \vec{p} and an energy $i\frac{2\pi}{\beta}(n + \frac{1}{2})$ corresponds to

$$\frac{i}{i\frac{2\pi}{\beta}(n + \frac{1}{2}) - \epsilon_{\vec{p}}} \quad (3.4)$$

with n an integers; a free boson propagator, represented by a dashed line, with a momentum \vec{p} and an energy $i\frac{2\pi}{\beta}n$ corresponds to

$$\frac{i}{i\frac{2\pi}{\beta}n - \omega_{\vec{p}}}; \quad (3.5)$$

a vertex with two incoming electrons and one outgoing boson corresponds to $-ig$ and that with two outgoing electrons and one incoming boson to ig . The energy and momentum are conserved at each vertex. A loop corresponds to a sum and an integral

$$\frac{i}{\beta} \sum_l \int \frac{d^2q}{(2\pi)^2}$$

with l the integer labeling the Matsubara energy of a chosen line of the loop and \vec{q} the momentum of that line. A minus sign is associated with a fermionic loop. All arrows in the diagrams follow the charge flow.

The electron self-energy to the one-loop order is given by i times the amputated part of the diagram in Fig. 2a, i.e.

$$\Sigma_n(\vec{p}) = i\frac{i}{\beta}(-ig)ig \sum_l \int \frac{d^2q}{(2\pi)^2} \left[\frac{i}{i\frac{2\pi}{\beta}l - \omega_{\vec{q}}} \right] \left[\frac{i}{i\frac{2\pi}{\beta}(l - n - \frac{1}{2}) - \omega_{\vec{q}-\vec{p}}} \right]$$

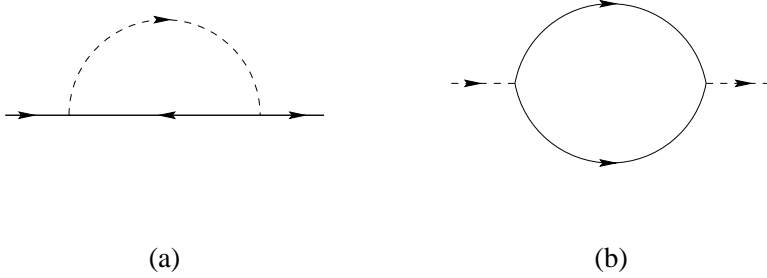


Figure 2. The one-loop diagrams for the self-energy of an electron (a) and the self-energy of a boson (b).

$$= g^2 \int \frac{d^2 q}{(2\pi)^2} \frac{N_b(\vec{q}) + N_f(\vec{q} - \vec{p})}{i\frac{2\pi}{\beta}(n + \frac{1}{2}) - \omega_{\vec{q}} - \epsilon_{\vec{q} - \vec{p}}}, \quad (3.6)$$

where N_b and N_f are boson and fermion distribution functions given by

$$N_b(\vec{p}) = \frac{1}{e^{\beta\omega_{\vec{p}}} - 1} \quad (3.7)$$

and

$$N_f(\vec{p}) = \frac{1}{e^{\beta\epsilon_{\vec{p}}} + 1} \quad (3.8)$$

respectively. With the Matsubara energy $i\frac{2\pi}{\beta}(n + \frac{1}{2})$ replaced by $p_0 + i0^+$, we obtain the retarded self-energy function

$$\Sigma(p_0, \vec{p}) = g^2 \int \frac{d^2 q}{(2\pi)^2} \frac{N_b(\vec{q}) + N_f(\vec{q} - \vec{p})}{p_0 - \omega_{\vec{q}} - \epsilon_{\vec{q} - \vec{p}} + i0^+}. \quad (3.9)$$

If the bosonic chemical potential $-\delta$ were zero, the integration over \vec{q} would be logarithmically divergent. Therefore, in the limit $\delta \rightarrow 0$, we expect

$$\Sigma(p_0, \vec{p}) \rightarrow \frac{\bar{\Delta}^2}{p_0 + \epsilon_{\vec{p}}} \quad (3.10)$$

with

$$\bar{\Delta}^2 = \frac{g^2 m_b \kappa T}{2\pi} \ln \frac{\kappa T}{\delta}. \quad (3.11)$$

The right hand side of (3.10) is of the same form as (2.14) and a perfect gap emerges. With a moderate logarithmic factor, the gap becomes a pseudo one as smeared by the imaginary part of $\Sigma(p_0, \vec{p})$. The integration in (3.9) can be carried out analytically in the situation $\mu \gg \kappa T$ and $\mu \gg \epsilon_{\vec{p}}$ and $\mu \gg p_0$. The result reads

$$\Sigma(p_0, \vec{p}) = g^2 \frac{m_b}{2\pi} \left\{ \frac{\kappa T}{\sqrt{4r\mu\delta + (p_0 + \epsilon_{\vec{p}} - \delta)^2}} \right\} \text{sign}(p_0 + \epsilon_{\vec{p}} - \delta)$$

$$\begin{aligned} & \times \ln \left[\frac{\sqrt{4r\mu\delta + (p_0 + \epsilon_{\vec{p}} - \delta)^2} + |p_0 + \epsilon_{\vec{p}} - \delta|}{\sqrt{4r\mu\delta + (p_0 + \epsilon_{\vec{p}} - \delta)^2} - |p_0 + \epsilon_{\vec{p}} - \delta|} - i\pi \right] \\ & - \frac{\ln r}{r-1} + \frac{1}{2} \sqrt{\frac{\pi\kappa T}{r\mu}} \left[f(e^{-\beta(p_0 - \delta)}) - i f(e^{\beta(p_0 - \delta)}) - i\zeta\left(\frac{1}{2}\right) \right] \Big\}, \quad (3.12) \end{aligned}$$

where the function f is defined as

$$f(z) = \frac{2}{\sqrt{\pi}} \int_0^\infty dx \sqrt{x} \frac{ze^{-x}}{(1+ze^{-x})^2}, \quad (3.13)$$

$r = m_b/m_f$ and $\zeta(1/2) = -1.4604$. For \vec{p} on the Fermi surface, $p = p_F$, $\epsilon_{\vec{p}} = 0$ and we find that $\Sigma(p_0, \vec{p})|_{p=p_F} = u(p_0) + iv(p_0)$ where

$$\begin{aligned} u(p_0) &= g^2 \frac{m_b}{2\pi} \left[\frac{\kappa T \text{sign}(p_0 - \delta)}{\sqrt{4r\mu\delta + (p_0 - \delta)^2}} \ln \frac{\sqrt{4r\mu\delta + (p_0 - \delta)^2} + |p_0 - \delta|}{\sqrt{4r\mu\delta + (p_0 - \delta)^2} - |p_0 - \delta|} \right. \\ &\quad \left. - \frac{\ln r}{r-1} + \frac{1}{2} f(e^{-\beta(p_0 - \delta)}) \sqrt{\frac{\pi\kappa T}{r\mu}} \right] \quad (3.14) \end{aligned}$$

and

$$v(p_0) = -g^2 \frac{m_b}{2\pi} \left[\frac{\pi\kappa T}{\sqrt{4r\mu\delta + (p_0 - \delta)^2}} \right.$$

with

$$\left. + \frac{1}{2} \left(f(e^{\beta(p_0 - \delta)}) + \zeta\left(\frac{1}{2}\right) \right) \sqrt{\frac{\pi\kappa T}{r\mu}} \right]. \quad (3.15)$$

The spectral function at the Fermi surface is

$$A(p_0, \vec{p})|_{p=p_F} = \frac{1}{\pi} \text{Re} \frac{i}{p_0 - u(p_0) - iv(p_0) + u(\delta)}, \quad (3.16)$$

where we have renormalized the chemical potential in (3.16) by subtracting the constant term $u(\delta)$. The function $A(p_0, \vec{p})$ on the Fermi surface is plotted in Fig.3 for $\ln \frac{\kappa T}{\delta} = 8, 6$ and 4 respectively. The opening of a pseudo gap with increasing $\ln \kappa T/\delta$ is clearly shown.

3.2 A resummation of higher order diagrams

The validity of the perturbative results for $\Sigma(p_0, \vec{p})$ requires both $\hat{g}^2 \ll 1$ and $\hat{g}^2 \ln \frac{\kappa T}{\delta} \ll 1$. Nonperturbative effects will enter the game if the second inequality fails. In what follows, we shall examine

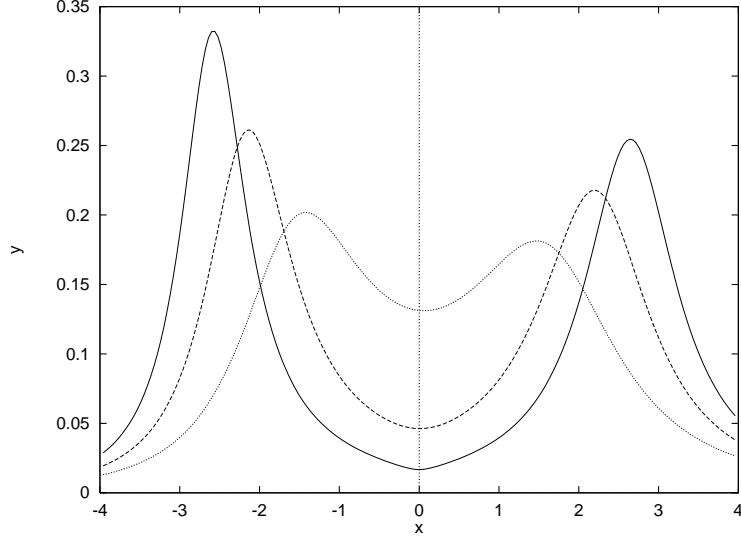


Figure 3 The spectral function at $\epsilon_{\vec{p}} = 0$, with $\beta\mu = 10$, $r = 2$ and $g^2 m_b \beta / 2\pi = 1$. The solid line corresponds to $\ln \kappa T / \delta = 8$, the dashed line to $\ln \kappa T / \delta = 6$ and the dotted line to $\ln \kappa T / \delta = 4$, where $x = p_0 / \kappa T$ and $y = A(p_0, \vec{p})|_{p=p_F} \kappa T$.

the higher order diagrams and derive an expression which can be extended to the region $\hat{g}^2 \ll 1$ but $\hat{g}^2 \ln \frac{\kappa T}{\delta} \sim 1$

A diagrams of an electron propagator to an arbitrary order consists of at least a string of electron lines, referred to as the main string, joining the initial and the final states. A number of vertices has to be attached to this line. In what follows, a vertex with an outgoing boson line will be referred to as a source and that with an incoming boson line will be referred to as a sink. On account of the charge conservation, there should be an even number of vertices with sources and sinks alternatively attached to the main string. Without decorating the boson lines, there are no electron lines outside the main string. Unlike the super phase (Fig. 1), in which the boson lines all terminated at the condensate, a boson line emitted from a source can land at any sink of the diagram. Therefore there are $N!$ such diagrams to the $2N$ -th order in g and N loops in each diagram. Such an expansion to 6th order in g is displayed in Fig. 4. Each loop contains a boson leaving the main string and then coming back. The Matsubara energies of these bosons are denoted by $i\frac{2\pi}{\beta}l_m$ ($m = 1, 2, \dots, N$) with l_m integers and the corresponding momenta by \vec{q}_m . l_m 's are to be summed and \vec{q}_m 's are to be integrated. The leading divergence as $\delta \rightarrow 0$ comes from the integrals over \vec{q}_m 's of the term with $l_1 = l_2 = \dots = l_N = 0$, where each momentum integral over \vec{q}_m is logarithmically divergent.

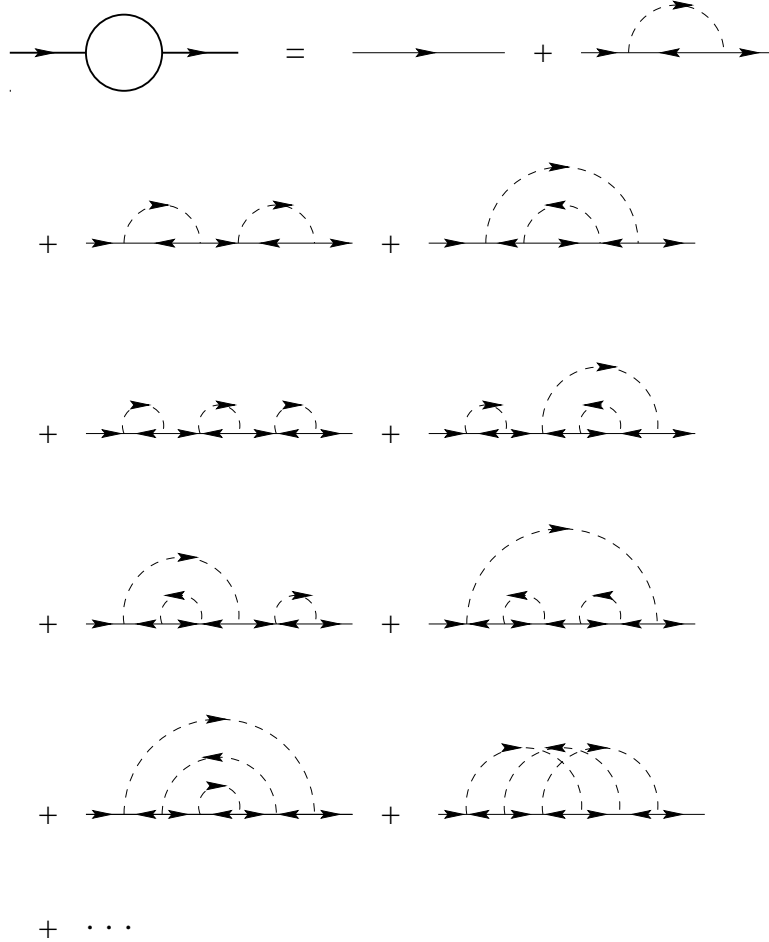


Figure 4. The diagrammatic expansion of the electron propagator in the normal phase.

For a tiny δ , each integral remains dominated by the lower limit, and contribute the amplitude of the diagram a factor $\ln \frac{\Lambda}{\delta} \gg 1$ with Λ a cutoff energy $\sim \kappa T$. To the leading order of these logarithms, the terms with some of l_m 's nonzero can be dropped and the deviation of the momentum of an internal electron line along the main string from the external momentum \vec{p} due to the boson emissions and absorptions can be neglected. Collecting all the fermionic propagators and vertices with such an approximation, we find that all $2N$ -th order diagrams contribute equally to the full electron propagator, $S_n(\vec{p})$, a term

$$\frac{i}{i\nu_n - \epsilon_{\vec{p}}} (-)^N \left(\frac{\bar{\Delta}^2}{\nu_n^2 + \epsilon_{\vec{p}}^2} \right)^N, \quad (3.17)$$

where $\nu_n = \frac{2\pi}{\beta}(n + \frac{1}{2})$ and

$$\bar{\Delta}^2 = g^2 \frac{m_b \kappa T}{2\pi} \ln \frac{\Lambda}{\delta} = 2\hat{g}^2 \frac{m_b}{m_f} \frac{\nu \kappa T}{\pi} \ln \frac{\Lambda}{\delta}$$

with \hat{g} defined by (2.5). On summing over N , we obtain

$$S_n(\vec{p}) = \frac{i}{i\nu_n - \epsilon_{\vec{p}}} F\left(\frac{\bar{\Delta}^2}{\nu_n^2 + \epsilon_{\vec{p}}^2}\right), \quad (3.18)$$

where function F is given by the asymptotic series

$$F(\zeta) \sim \sum_N (-)^N N! \zeta^N, \quad (3.19)$$

which is formally Borel summable [9] (It is advantageous in this case not to distinguish the one particle irreducible diagrams with the reducible ones). On substituting

$$N! = \int_0^\infty dt t^N e^{-t} \quad (3.20)$$

into (3.19) and interchanging the order of the integration and the summation, we find

$$F(\zeta) = \int_0^\infty dt \frac{e^{-t}}{1 + \zeta t} = -\frac{1}{\zeta} e^{\frac{1}{\zeta}} \text{Ei}\left(-\frac{1}{\zeta}\right), \quad (3.21)$$

where the function Ei is the exponential integral defined in [10]

$$\text{Ei}(z) \equiv \int_{-\infty}^z dt \frac{e^t}{t} \quad (3.22)$$

with $\arg(-z) < \pi$. $\text{Ei}(z)$ is analytic on the z -plane cut along the positive real axis with the discontinuity across the cut given by

$$\text{Ei}(x + i0^+) - \text{Ei}(x - i0^+) = -2\pi i. \quad (3.23)$$

The asymptotic expansion with a large $|z|$ or a small $|z|$ are given respectively by

$$\text{Ei}(z) = \begin{cases} \gamma + \ln(-z) + \sum_{n=1}^{\infty} \frac{z^n}{n!n} & \text{for } |z| \ll 1; \\ \frac{e^z}{z} \sum_{n=0}^{\infty} \frac{n!}{z^n} & \text{for } |z| \gg 1 \end{cases} \quad (3.24)$$

with γ the Euler constant.

Replacing the imaginary energy $i\nu_n$ by $p_0 + i0^+$, we obtain the retarded electron propagator:

$$S_R(p_0, \vec{p}) = i \frac{p_0 + \epsilon_{\vec{p}}}{\bar{\Delta}^2} e^{-\frac{p_0^2 - \epsilon_{\vec{p}}^2}{\bar{\Delta}^2}} \text{Ei}\left(\frac{(p_0 + i0^+)^2 - \epsilon_{\vec{p}}^2}{\bar{\Delta}^2}\right), \quad (3.25)$$

which returns to the free propagator in the limit $\bar{\Delta} \rightarrow 0$, i.e.

$$\lim_{\bar{\Delta} \rightarrow 0} S_R(p_0, \vec{p}) = \frac{i}{p_0 - \epsilon_{\vec{p}} + i0^+}. \quad (3.26)$$

The self-energy function extracted from (3.22) according to (2.13) reads

$$\Sigma(p_0, \vec{p}) = \frac{\bar{\Delta}^2}{p_0 + \epsilon_{\vec{p}}} \left[z - z \frac{d}{dz} \ln \text{Ei}(z) \right] \quad (3.27)$$

with $z = \frac{p_0^2 - \epsilon_{\vec{p}}^2}{\bar{\Delta}^2}$, which agrees with the one-loop result if $\hat{g}^2 \ll \hat{g}^2 \ln \frac{\kappa T}{\delta} \ll 1$.

For a fixed \vec{p} , $S_R(p_0, \vec{p})$ is an analytic function on the p_0 plane with two cuts running from $|\epsilon_{\vec{p}}|$ to ∞ and from $-|\epsilon_{\vec{p}}|$ to $-\infty$. The spectral function is given by the discontinuity across the cuts. It follows from (3.23) and (3.25) that

$$\begin{aligned} A(p_0, \vec{p}) &= \frac{1}{\pi} \text{Re} S_R(p_0 + i0^+, \vec{p}) \\ &= \begin{cases} 0, & \text{for } |p_0| < |\epsilon_{\vec{p}}|; \\ \frac{|p_0 + \epsilon_{\vec{p}}|}{\bar{\Delta}^2} e^{-\frac{p_0^2 - \epsilon_{\vec{p}}^2}{\bar{\Delta}^2}}, & \text{otherwise.} \end{cases} \end{aligned} \quad (3.28)$$

The dependence of $A(p_0, \vec{p})$ of (3.28) on the coupling constant g in nonperturbative. On the Fermi surface, $\epsilon_{\vec{p}} = 0$, we have

$$A(p_0, \vec{p})|_{p=p_F} = \frac{|p_0|}{\bar{\Delta}^2} e^{-\frac{p_0^2}{\bar{\Delta}^2}}. \quad (3.29)$$

Two peaks at $p_0 = \pm \bar{\Delta}/\sqrt{2}$ together with a depletion of states at the Fermi level $p_0 = 0$ corresponding to a pseudo-gap emerge.

4. Comments

In this final section, we shall comments on the validity of our results for a realistic system and its relation with known results in the literature.

The electron self-energy function in the boson-fermion model has been investigated in [11] and a pseudo-gap was found in $D = 1$ and 2 by numerical solutions of the self-consistent equations for $\Sigma(p_0, \vec{p})$. The approach taken in this article is purely analytical with emphasis on the quasi-2D nature of the crystal structure. The one-loop result shows the trend of a pseudo-gap when the logarithmic factor $\ln \frac{\kappa}{\delta}$ becomes sizable and the resummation of the diagrams in Fig. 4 gives the nonperturbative effect when the logarithmic factor becomes dominant. We notice that the entangled diagrams, e.g. the last one of Fig. 4, which is often neglected in the self-consistent method, contribute equally as the others to the leading order of the logarithm. Nevertheless, the result as to the existence of a pseudo-gap of the present work agrees with that of [11] qualitatively.

The boson-fermion model is a phenomenological one, in which bosons are regarded as elementary. In a realistic system, bosons correspond to a pair of electrons and do not represent new degrees of freedom. This is not a serious problem as long as the charge density is not too high to cause substantial overlapping among the pairs. A theorem proved in [12] states that for any fermionic Hamiltonian, there exist an equivalent boson-fermion Hamiltonian with the elementary bosons of the latter correspond to the fermion pairs of the former. For a Hubbard like model with an on-site attraction and a nearest neighbor repulsion, the low density behavior is indeed described by the boson-fermion model.

Although the motion of electrons and pairs in the $x - y$ plane is assumed to be in continuum, the result will not be changed if we replace the motion in $x - y$ plane by lattice hopping. Furthermore, the model Hamiltonian (2.1) can also accommodate a momentum dependent coupling g , say

$$g \propto \hat{p}_x^2 - \hat{p}_y^2, \quad (4.1)$$

which results a pseudo-gap with d -wave character.

In the perturbative expansion (3.17), all boson propagators are kept undecorated. The decorations come in two ways: One is to replace the bare boson propagators by the dressed ones and the other is to include the scattering diagrams of these bosons. Both require

fermion loops in addition to the main string of fermion lines under discussion.

The dressing of the boson propagator is through the self-energy function $\Pi_n(\vec{p})$ defined at momentum \vec{p} and Matsubara energy $i\frac{2\pi n}{\beta}$. The one loop diagram for $\Pi_n(\vec{p})$ is depicted in Fig. 2b. We find, to that order and $n = 0$ that

$$\Pi_n(\vec{p}) = a + bp^2 \quad (4.2)$$

as $\vec{p} \rightarrow 0$ with a and b functions of T and μ . The result is believed to be true in multi-loops. Since the contribution to (3.14) comes only from the boson propagator with zero Matsubara energy and low momentum, the effect of the boson self-energy is merely a renormalization. The results of the last section is not modified if we regard m_b and δ being renormalized quantities.

The diagrams with boson scattering look problematic and the one of such diagrams to the lowest order in g is shown in Fig. 5a.

A naive power counting indicates a linear divergence in the limit $\delta \rightarrow 0$. This however can be eliminated on summing over the diagrams with repeated scatterings between two bosons as is shown in Fig. 5b-c. Our result will survive if this is also true for multi-boson scatterings.

The Coulomb interaction has been left out throughout the discussions. Strictly speaking, the Coulomb interaction is perturbative only if the inter-particle distance is short compared with the Bohr radius [13]. Therefore, the results of the preceding section would be unaffected in a hypothetical situation when the charge density is high enough and the bosons are truly elementary. The situation with the real materials is, however, not in the perturbative region at all. On the other hand, the shielding of the Fermi sea truncates the long range tail of the direct Coulomb force and there are possibilities that our results survive. Diagrammatically, inclusion of the Coulomb interaction amounts to decorate the electron and fermion propagators and the boson-fermion vertices and to add scattering diagrams between electron and bosons. As long as the Fermi-liquid behavior of electron spectrum and the low momentum behavior of the boson spectrum are not modified by Coulomb interactions alone, our result remain qualitatively intact.

Technically, the most drastic step leading to (3.25) is the Borel summation of the perturbative series (3.18). Is the sum unique? An asymptotic expansion of a given function $F(\zeta)$, i.e.

$$F(\zeta) \sim \sum_n a_n \zeta^n, \quad (4.3)$$

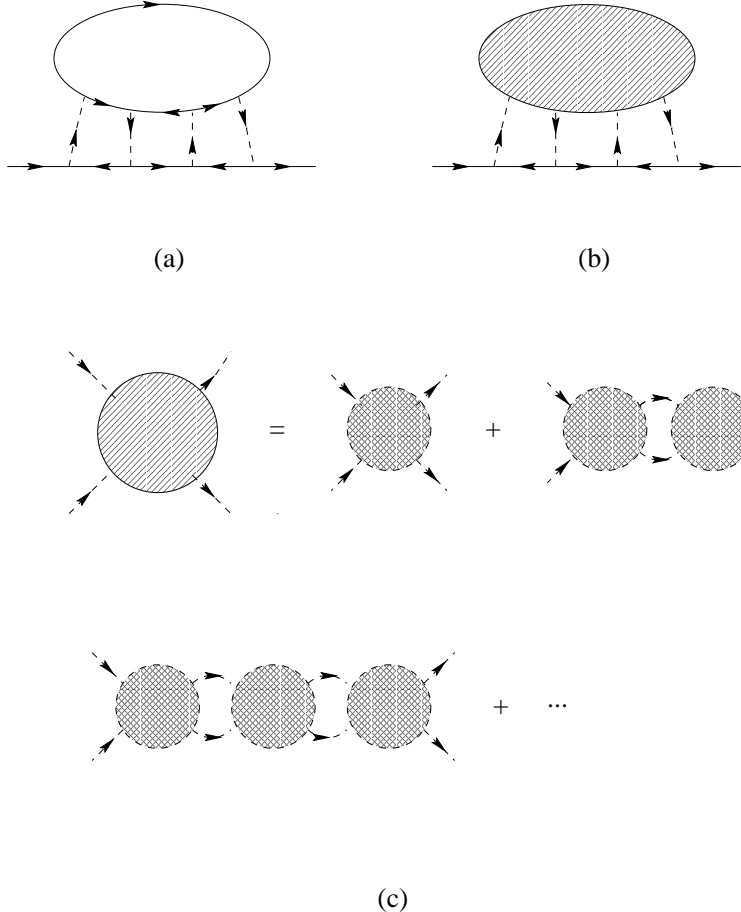


Figure 5. (a) The lowest order diagram of the electron propagator with scattering of virtual bosons; (b) The propagator diagram with the scattering between the two virtual bosons to all orders; (c) The expansion of the shaded part of (b). A cross-shaded bubble is a two particle irreducible part.

may well be the asymptotic expansion of another function, say $F(\zeta) + e^{-\frac{1}{\zeta}}$. Therefore the sum of an asymptotic series is in general nonunique unless certain conditions are preimposed on the sum. According to the Watson theorem in [9], the sufficient conditions for the Borel sum to be a unique function $F(\zeta)$ which produce the asymptotic expansion of the right hand side of (4.3) are: 1) $F(\zeta)$ has to be analytic within the region D defined by $|\zeta| < r$ and $|\arg(\zeta)| < \frac{\pi}{2} + \alpha$ with $r > 0$ and $\alpha > 0$; 2) $|a_n| = O(n! \sigma^n)$; with $\sigma > 0$; 3)

$$|F(\zeta) - \sum_{n=0}^N a_n \zeta^n| = O((n+1)! \sigma^{n+1} r^{n+1}). \quad (4.4)$$

uniformly within D . It follows from the rigorous spectral representation of the fermion propagator that the condition 1) is indeed satisfied if we identify z with $\bar{\Delta}^2/(\nu_n + \epsilon_{\vec{p}})$ and the coefficients of the perturbation series (3.18) meet 2). The condition 3) is difficult to justify nonperturbatively. Furthermore, each term in (3.18) is only a part of the perturbation in terms of g , since only the leading logarithmic term is reserved. Therefore the rigorous mathematical justification of the Borel sum (3.18) remains open.

Acknowledgement

The author is indebted to Mr. O. Tchernyshyov for interesting him with this problem and for stimulating conversations. He is grateful to Professor N. N. Khuri for his critical reading of the manuscript. He would also like to thank Professor V. P. Nair for discussions and to thank Dr. James Liu for advice. This work is supported in part by the U. S. Department of Energy under Contract Grant DE-FG02-91ER40651.

REFERENCES

1. A. G. Loeser, D. S. Dessau and Z. X. Shen, *Physica* **C263**, 208 (1996); H. Ding, *et. al.*, *Nature*, **Vol. 382**, 51 (1996).
2. N. P. Ong, *et. al.*, "Charge Transport Properties of Cuprate Superconductors", in "*High- T_C Superconductivity and C_60 Family*", Proceeding of CCAST Symposium/Workshop, ed. S. Q. Feng and H. C. Ren, Gordon and Breach Pub. Inc., 1994; S. Uchida, "Optical Spectra of High- T_C Superconductors", *ibid.*
3. R. Friedberg and T. D. Lee, *Phys. Lett.* **A138**, 423 (1989); *Phys. Rev. B* **40**, 6745 (1989).
4. Y. Uemura, *et. al.*, *Phys. Rev. Lett.* **62**, 2317 (1989); Y. Uemura, "Energy Scales of High T_C Cuprates, Doped-Fullerenes, and Other Exotic Superconductors", in "*High- T_C Superconductivity and C_60 Family*", Proceeding of CCAST Symposium/Workshop, ed. S. Q. Feng and H. C. Ren, Gordon and Breach Pub. Inc., 1994.
5. R. Friedberg, T. D. Lee and H. C. Ren, *Phys. Lett. A* **152**, 423 (1991)
6. R. Micnas, J. Ranninger and S. Robaszkiewicz, *Rev. Mod. Phys.* **62**, 113 (1990), and the references therein.
7. R. Friedberg, T. D. Lee and H. C. Ren, *Phys. Lett. A* **152**, 417 (1991)
8. G. Baym and N. D. Mermin, *J. Math. Phys.*, **2**, 232(1961)
9. G. Hardy, *Divergent Series*, Oxford University Press, New York (1949).
10. N. N. Lebedev, *Special Functions and Their Applications*, Trans. R. Silverman, Dover Pub. Inc., 1972

11. J. Ranninger, J. M. Robin and M. Eschrig, *Phys. Rev. Lett.*, **74**, 4027 (1995).
12. R. Friedberg, T. D. Lee and H. C. Ren, *Phys. Rev. B* **50**, 10190 (1994).
13. M. Gell-Mann and K. A. Brueckner , *Phys. Rev.* **106**, 364, (1957).